EFFECT OF TAPERING ON OPTICAL GUIDING AND SIDEBAND GROWTH IN A FINITE-PULSE FREE-ELECTRON LASER

B. Hafizi*, A. Ting, P. Sprangle and C. M. Tang

Plasma Theory Branch
Plasma Physics Division
Naval Research Laboratory
Washington, DC 20375-5000

Abstract

The development of an optical pulse of finite axial extent is studied by means of a numerical code. It is found that increasing the tapering rate reduces refractive guiding, causing the optical wavefronts to become more convex, thus spreading the optical field into a larger cross-section. This increases the output power and efficiency. Concomitant with this, there is a significant reduction in the sideband modulation of the optical field.

I. Introduction

We present the results from a numerical study of a high-current (~ kA), high-power (~ GW), short wavelength (~ μm), tapered-wiggler free-electron laser (FEL). The results indicate that tapering, in addition to enhancing the extraction efficiency, has the further benefit of improving the quality of the output by suppressing sideband modulation of the optical field. The results are used to illustrate the transition between refractive guiding and gain focusing as the tapering rate is varied.

II. Formulation

The vector potential of the optical field is given by

$$\mathbf{A}_s = \frac{A}{2}\exp\left[i\left(\frac{\omega}{c}z - \omega t\right)\right]\mathbf{e}_x + \text{c.c.},$$

where A is the slowly-varying envelope, ω is the radian frequency, and $\mathbf{e}_x$ is the unit vector along the x axis. We assume that A may be expanded as

$$a(r,z,t) = \sum_{n=0}^{\infty} a_n(z,t)\, L_n\left(2r^2/r_s^2\right) \times \exp\left[-(1 - i\alpha)\, r^2/r_s^2\right], \qquad (1)$$

where $a = |e|A/mc^2$, $-|e|$ is the charge on an electron of rest-mass m, and L_n is the Laguerre polynomial of order n. In (1) $r_s(z,t)$ is the spot-size, $\alpha(z,t)$ is proportional to the curvature of the optical field, and $\{a_n(z,t)\}$ are the transverse optical mode coefficients. Substituting (1) into the well-known parabolic wave equation and employing the source-dependent expansion technique of Ref. 1, one obtains the set of equations given in Ref. 2 for the evolution of r_s, α, and $\{a_n\}$. The code includes betatron motion in a planar wiggler with parabolic pole faces. [3] The synchrotron motion is generalized from that given in Ref. 2 by the addition of the betatron terms in the equation for the electron phase.

The electron beam is taken to have a parabolic density distribution in the transverse plane and a Gaussian distribution in the transverse velocities. The normalized edge emittance for such a distribution may be defined by:

$$\varepsilon_x = 2\sqrt{6}\left[\langle x^2\rangle\langle\gamma^2\beta_x^2\rangle - \langle x\gamma\beta_x\rangle^2\right]^{1/2},$$

and similarly for ε_y. Here <...> indicates an average over the entire beam.

The relativistic factor for a synchronous electron with no betatron motion is given by $\gamma_r^2 = (\omega/2ck_w)(1 + a_w^2/2)$, where $a_w = |e|B_w/k_w mc^2$, B_w is the induction and $2\pi/k_w$ is the wiggler period. The form of tapering employed in the computations is obtained simply by prescribing a constant rate of decrease of energy $d\gamma_r/dz < 0$ for a synchronous electron.

The parameters for the computations presented herein are listed in Table I. The effective energy spread due to emittance is given by

$$\left[\frac{\delta\gamma_r}{\gamma_r}\right]_{\text{emit}} = \frac{\left(\varepsilon_x^2 + \varepsilon_y^2\right)/2}{\left(2r_{bo}\right)^2\left(1 + a_w^2/2\right)^2},$$

where r_{bo} is the electron beam radius. The full ponderomotive bucket height for electrons on axis is given by

$$\left[\frac{\delta\gamma_r}{\gamma_r}\right]_{\text{bucket}} = \left\{\frac{2a_w|a|f_B}{\left(1 + a_w^2/2\right)} \times \left[\cos\xi_r - \left(\frac{\pi}{2}\operatorname{sgn}\xi_r - \xi_r\right)\sin\xi_r\right]\right\}^{1/2},$$

where $a = |a|\exp(i\phi)$, $\xi_r = \psi_r + \phi$, and the phase $\psi_r = (\omega/c + k_w)z - \omega t$ of the synchronous electron is related to the rate of change of γ_r in the tapered FEL by

$$\frac{d\gamma_r}{dt} = -\frac{a_w|a|\omega f_B}{2\gamma_r}\sin(\psi_r + \phi).$$

Table I. Parameters for a high-power, rf-linac FEL

Electron Beam	
Energy, γmc^2	175 MeV
Current, I_b	450 A
Normalized edge emittance, $\varepsilon_x = \varepsilon_y$	153 mm-mrad
Radius, r_{bo}	1 mm
Wiggler	
Pulse length	6.7 ps
Induction, B_w	6.4 kG
Period, $2\pi/k_w$	4.7 cm
Length	42 m
Input Radiation	
Wavelength, $2\pi c/\omega$	1 μm
Spot size, $r_s(0)$	1.25 mm
Pulse length (FWHM)	31.4 ps
Peak input power	450 MW

Table II lists the full bucket height for the various tapering rates $d\gamma_r/dz \simeq c^{-1}\, d\gamma_r/dt$ employed in the computations. Note that for the input power of 450 MW essentially all the electrons are initially trapped. Also listed in Table II are the initial resonance phases ξ_r.

Table II. Resonance phases and tapering rates

$d\gamma_r/dz$ (m^{-1})	Initial Resonance Phase ξ_r(°)	Full bucket height $[\delta\gamma_r/\gamma_r]_{bucket}$ (%)	Energy spread due to emittance $[\delta\gamma_r/\gamma_r]_{emit}$ (%)
-0.1	2.5	0.96	
-0.3	7.6	0.89	
-0.5	12.7	0.82	
-0.7	17.9	0.75	
-0.9	23.3	0.67	0.12
-1.1	28.9	0.6	
-1.3	34.5	0.52	
-1.5	41.2	0.44	

III. Results and Discussion

Herein we shall present the results for two tapering rates only. The two cases discussed in detail suffice since there is a gradual change in the physical characteristics in going from one tapering rate to the next.

(a) Sideband Instability and Pulse Modulation

The tapering rate has a dramatic effect on the profile of the output optical pulse. This is illustrated rather well in Figs. 1 (a) and (b) which display the normalized radiation field amplitude $a_o(z)$ for the fundamental optical mode at the wiggler exit. The two cases correspond to initial resonance phases ξ_r = 2.5° and 34.8°. In the presence of the sidebands, the optical field will be modulated at a period λ_{mod} given by

$$\lambda_{mod} \simeq \left(\frac{1 + a_w^2/2}{2a_w|a_o|f_B}\right)^{1/2} \lambda.$$

Taking $|a| = 1.4\times10^{-4}$, one finds $\lambda_{mod} \simeq 0.09$ mm which is within 10% of the period of the prominent oscillations observed in Fig. 1(a). On the other hand, when the tapering rate $d\gamma_r/dt$ is sufficiently fast the synchrotron motion of the electrons is nonadiabatically distorted. This tends to suppress sideband growth. [2] For the parameters considered here and the tapering rate for Fig. 1(b), one finds that, if Ω_{syn} is the synchrotron frequency,

$$\left|\frac{d\gamma_r/dt}{\Omega_{syn}(\gamma - \gamma_r)}\right| \sim 1/5,$$

whence the synchrotron motion is marginally nonadiabatic. The distortion of the synchrotron motion is responsible for reduced sideband growth.

(b) Optical Guiding

Optical guiding may be shown to arise from two distinct features of the FEL mechanism. [4] Refractive guiding, which is described by the reactive (real) part of the refractive index, is due to the phase shift of light. A distinguishing characteristic of this type of guiding is that the optical wavefronts are plane under the conditions of perfect guiding. The other type of guiding, gain focusing, is described by the resistive (imaginary) part of the refractive index. In this case, under the conditions of perfect guiding, the wavefronts are convex, corresponding to the fact that there is a net power flow, due to diffraction, away from the electron beam.

Figure 2 shows $\alpha(z)$, which is proportional to the curvature of the wavefronts, at the end of wiggler. The significant feature of Fig. 2 is that the curvature is less for the less rapidly tapered case. In particular, in the vicinity of z = 1.2 mm in Fig. 2(a), the curvature is negative, indicating that the wavefronts in this region are in fact concave. On the other hand, in the case of rapid tapering, Fig. 2(b), the wavefronts are convex all through the pulse, indicating a flow of power away from electron beam throughout the pulse. Consistent with this, Fig. 3 indicates a larger spot size for the more rapidly tapered case.

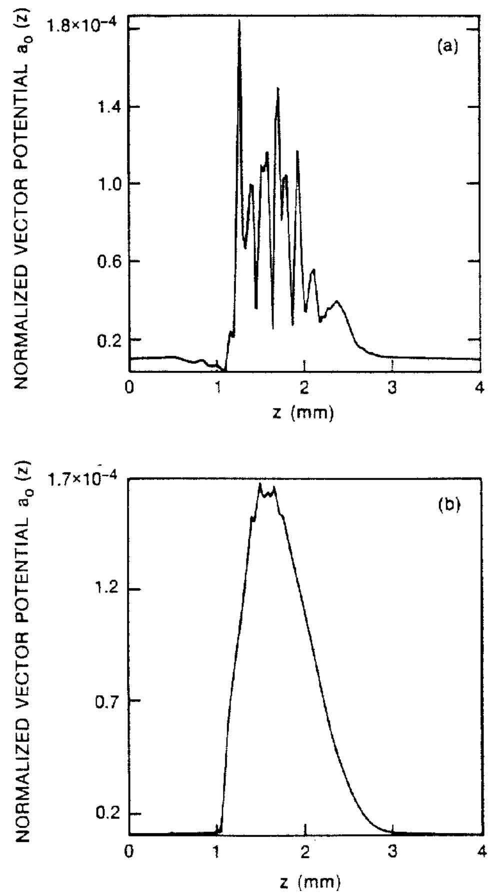

Fig. 1 Normalized vector potential of the fundamental optical mode $a_o(z)$ at the end of the wiggler. (a) slow tapering rate, initial resonance ξ_r = 2.5°; (b) rapid tapering rate, initial resonance phase ξ_r = 34.8°.

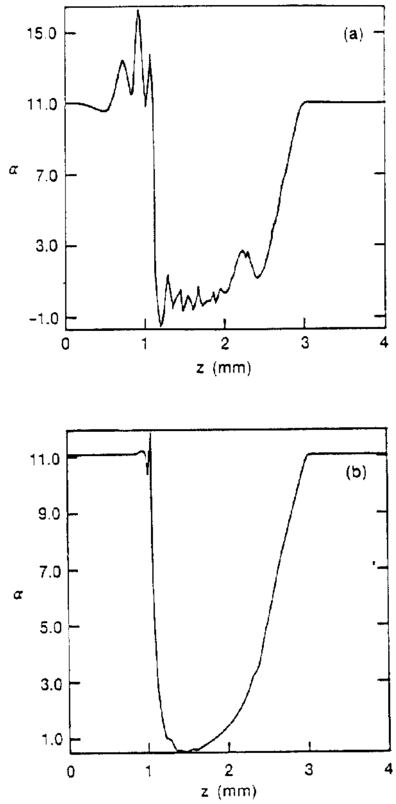

Fig. 2 Curvature α(z) at end of wiggler. (a) slow tapering rate; (b) rapid tapering rate

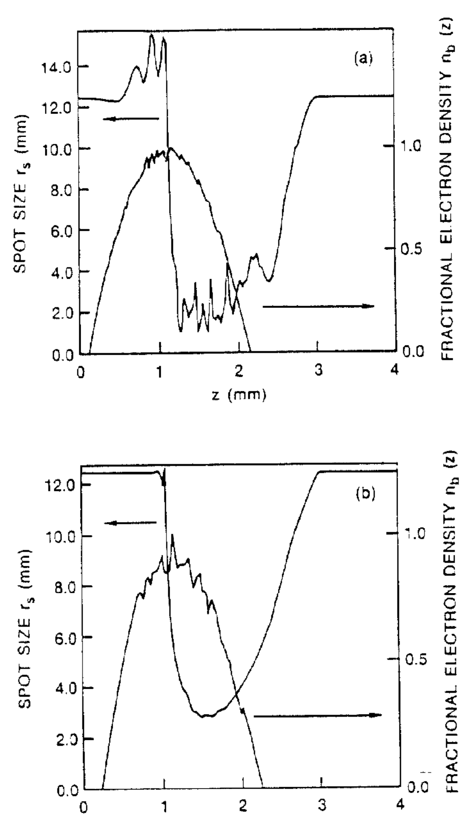

Fig. 3 Spot size $r_s(z)$ and fractional electron density $n_b(z)$ at end of wiggler. (a) slow tapering rate; (b) rapid tapering rate.

IV. Conclusions

Summarizing the results, it is found that in addition to enhancing the efficiency, tapering improves the quality of the output by suppressing sideband growth. Further, it is found that as the tapering rate is increased there is a gradual transition from a refractive-guiding regime to one where gain focussing dominates, with optical power diffracting laterally along the convex wavefronts. The increased transverse extent of the optical field, rather than an increase in the field amplitude is the major reason for efficiency enhancement as the tapering rate is increased.

Acknowledgment

This work was supported by ONR and SDIO through ONR.

References

[1] P. Sprangle, A. Ting and C. M. Tang, 'Radiation Focusing and Guiding with Application to the Free-Electron Laser,' Phys. Rev. Lett., Vol. 59, pp.202-205, 1987; 'Analysis of Radiation Focusing and Steering in the Free-Electron Laser by use of a Source-Dependent Expansion Technique,' Phys. Rev. A, Vol. 36, pp.2773-2781, 1987.

[2] B. Hafizi, A. Ting, P. Sprangle and C. M. Tang, 'Development of Sidebands in Tapered and Untapered Free-Electron Lasers,' Phys. Rev. A, Vol. 38, pp.197-203, 1988.

[3] E. T. Scharlemann, 'Wiggle Plane Focusing in Linear Wigglers,' J. Appl. Phys., Vol. 58, pp.2154-2161, 1985.

[4] E. T. Scharlemann, A. M. Sessler and J. S. Wurtele, 'Optical Guiding in a Free-Electron Laser,' Nucl. Instrum. Methods Phys. Res. A, Vol. 239, pp.29-35, 1985.

*Permanent address: Science Applications Intl. Corp., McLean, VA